Carbohydrate Polymers 98 (2013) 465–469

Contents lists available at SciVerse ScienceDirect

Carbohydrate Polymers

journal homepage: www.elsevier.com/locate/carbpol

Short communication

Nanocrystalline cellulose with various contents of sulfate groups

M.I. Voronova*, O.V. Surov, A.G. Zakharov

Federal Government Institution of Sciences, G.A. Krestov Institute of Solution Chemistry of the Russian Academy of Sciences, Akademicheskaya St., 1, Ivanovo 153045, Russian Federation

ARTICLE INFO

Article history:
Received 1 March 2013
Received in revised form 31 May 2013
Accepted 4 June 2013
Available online 20 June 2013

Keywords:
Nanocrystalline cellulose
Hydrolysis
Surface morphology

ABSTRACT

Properties of films derived from aqueous nanocrystalline cellulose dispersions by water evaporation depend on concentration of sulfate groups. Namely type of thermodestruction and surface morphology change as a function of contents of sulfate groups. Surface roughness increases and water adsorption enhances with increasing sulfate groups content particularly at high relative pressure.

1. Introduction

To produce nanocrystalline cellulose (NCC) means to remove all non-cellulose components and amorphous areas and to isolate cellulose crystallites formed during biosynthesis. There are various techniques to isolate cellulose crystallites; namely fermentation and acid hydrolysis by different mineral acids. However, only controlled hydrolysis with sulfuric acid (Habibi, Lucia, & Rojas, 2010; Lima & Redouane, 2004) (as a result of cellulose hydroxyl group esterification) allows to produce stable suspensions mainly due to grafting sulfate groups in a random way distributed on cellulose crystallite surface and consequently electrostatic repulsion of negatively charged particles.

The effect of hydrolysis conditions on NCC properties has been studied in a number of papers (Dong, Revol, & Gray, 1998; Gu, Catchmark, Kaiser, & Archibald, 2013; Jiang, Esker, & Roman, 2010; Martínez-Sanz, Lopez-Rubio, & Lagaron, 2011; Rahimi & Behrooz, 2011; Wang, Ding, & Cheng, 2007). It has been demonstrated that the increase in hydrolysis time leads to proliferation of sulfate groups grafted on cellulose crystallite surface, adds the degree of crystallinity (Martínez-Sanz et al., 2011), diminishes NCC particle size in water suspension (Rahimi & Behrooz, 2011), increases specific surface and volume of the voids (Lu & Hsieh, 2012). The sulfur content reflects the surface charge of the particles and electrostatic interaction between them, and it is crucial to the characterization and understanding of material properties (Abitbol, Kloser, & Gray, 2013).

It is the charge at the surface of the particles and electrostatic interaction between them that are critical for NCC properties. Sulfate groups at the surface add NCC water suspension stability, and at the same time reduce the temperature of destruction (Wang et al., 2007).

It is the purpose of our analysis to investigate the effect of sulfate group content in NCC samples on the properties of the films obtained by evaporation of water from NCC water suspension.

2. Materials and methods

2.1. Materials

Use has been made of commercial cellulose (Cellulose, powder ~20 μm, Aldrich) as starting microcrystalline cellulose.

2.2. Producing of water dispersion of NCC

Water dispersions of whiskers have been obtained from microcrystalline cellulose (MCC) by the method described previously (Bondeson, Mathew, & Oksman, 2006). Water dispersion of whiskers was prepared by the acid hydrolysis of MCC (10 g/100 ml). The acid hydrolysis was carried out with sulphuric acid (H_2SO_4) solution 64 wt% under continuous agitation. NCC samples with various contents of sulfate groups were obtained by variation of hydrolysis temperature and time. After hydrolysis, the suspension was repeatedly washed by centrifugation until the pH of suspension reached constant. Then the samples were treated by ultrasound (Sonorex DT 100 Bandelin Germany) during 15 min. The yield of cellulose crystallites was 30–35%.

---

* Corresponding author. Tel.: +7 4932 336237; fax: +7 4932 336237.
E-mail address: miv@isc-ras.ru (M.I. Voronova).

0144-8617/$ – see front matter © 2013 Elsevier Ltd. All rights reserved.
http://dx.doi.org/10.1016/j.carbpol.2013.06.004

Table 1
Hydrolysis conditions and NCC samples characteristics.

	MCC	Sample 1	Sample 2	Sample 3	Sample 4
Hydrolysis conditions[a]					
Temperature (°C)		45	45	45	60
Hydrolysis time (min)		20	60	120	120
Characteristics of CNCs					
Total sulfur content (%)	0	0.25	0.33	0.51	0.82
Hydrodynamic diameter (nm)	20,000	36 382	34 278	40 256	67 318
Degree of polymerization	210	150	102	80	78
Crystallinity index	79.6	85.3	85.6	87.8	92.6
Crystalline dimension by (2 0 0) plane (nm)	7.1	6.8	7.1	7.4	8.2
Degradation temperature, $t_{\max}$ (°C)					
The first process	341	169	171	175	178 (208)
The second process		375	372	374	368

[a] H_2SO_4 concentration – 64%, MCC concentration – 10 g/100 ml, the time of processing in ultrasound bath – 15 min.

NCC-films were made by evaporation of water from aqueous dispersion with concentration 10 g/l at room temperature. 15 ml of this NCC suspension was filled into a 5 cm diameter Petri dish and allowed to evaporate over a few days at ambient temperature to yield an NCC film.

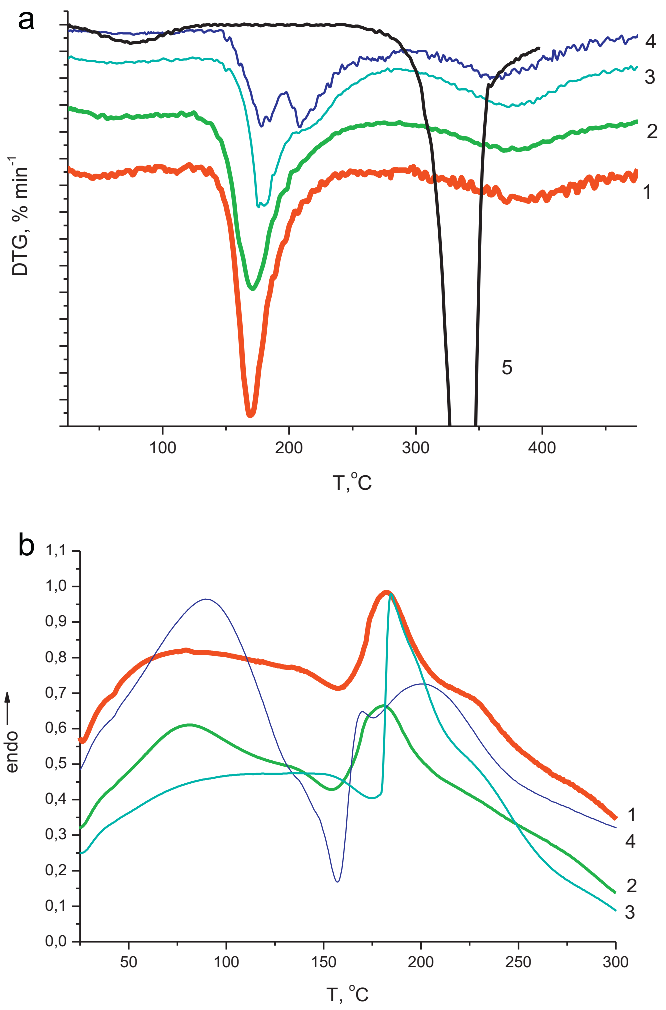

Fig. 1. DTG (a), DSC (b) curves for NCC (1–4) and MCC (5) samples. Numbering corresponds to that given in Table 1.

2.3. Characterization

Sulfate group content in the samples has been established by elemental analysis for sulfur by means of Flash EA – 1112 analyzer (Thermo Quest, Italia).

Atomic force microscopy (AFM) measurements were done with a Solver 47 Pro (cantilever NSG 11), resonance frequency of 150 kHz; scanning velocity 10 μm/s; amplitude of probe oscillation – 30–50 nm.

Dynamic light scattering (DLS) experiments were performed with a Zetasizer Nano-ZS (Malvern Instruments, Ltd.) in the range from 0.3 nm to 6 μm. Distribution of particle sizes in the microcrystalline cellulose (MCC) powder in the range of 0.3–300 μm was determined by means of laser particle size analyzer Analysette 22 (Fritsch GmbH, Germany).

X-ray diffraction analysis was performed using a Bruker D8 Advance diffractometer according to Bragg–Brentano scheme with Mo-Kα-radiation (λ = 0.071 nm). Crystallinity index (CI) of each sample was calculated by referring to diffraction intensity of crystalline and amorphous regions using the following empirical equation (Thygesen, Oddershede, Lilholt, Thomsen, & Stahl, 2005):

$$\mathrm{CI} = \frac{I_{2\ 0\ 0} - I_a}{I_{2\ 0\ 0}} \times 100, \qquad (1)$$

where $I_{2\,0\,0}$ is the intensity of a reflex 2 0 0, I_a is the intensity of an amorphous galo (minimum between the peaks 2 0 0 and 1 0 1). $I_{2\,0\,0}$ represents both crystalline and amorphous material while I_a represents amorphous material only. Crystal size was estimated using the Scherrer equation (Elazzouzi-Hafraoui et al., 2008; Kim, Eom, & Wada, 2010):

$$L = \frac{0.9\lambda}{\beta_{1/2}\cos\theta} \qquad (2)$$

where L is the crystal dimension perpendicular to the diffracting planes with Miller indices of *hkl*, λ is the wavelength of X-ray radiation and $\beta_{1/2}$ is the full width at half maximum of the diffraction peaks.

Temperature and heat effects of cellulose degradation were studied by means of differential scanning calorimeter DSC 204 F1 Foenix (Netzsch, Germany).

Dynamic thermogravimetric measurements were performed by TG 209 F1 Iris (Netzsch, Germany) using platinum crucibles in the atmosphere of dry argon at the flow rate 30 ml/min and the heating rate 10 K/min.

The degree of cellulose polymerization (DP) was assessed in terms of viscosity of its solution in cadoxene. Specific surface was determined in terms of low-temperature adsorption of nitrogen.

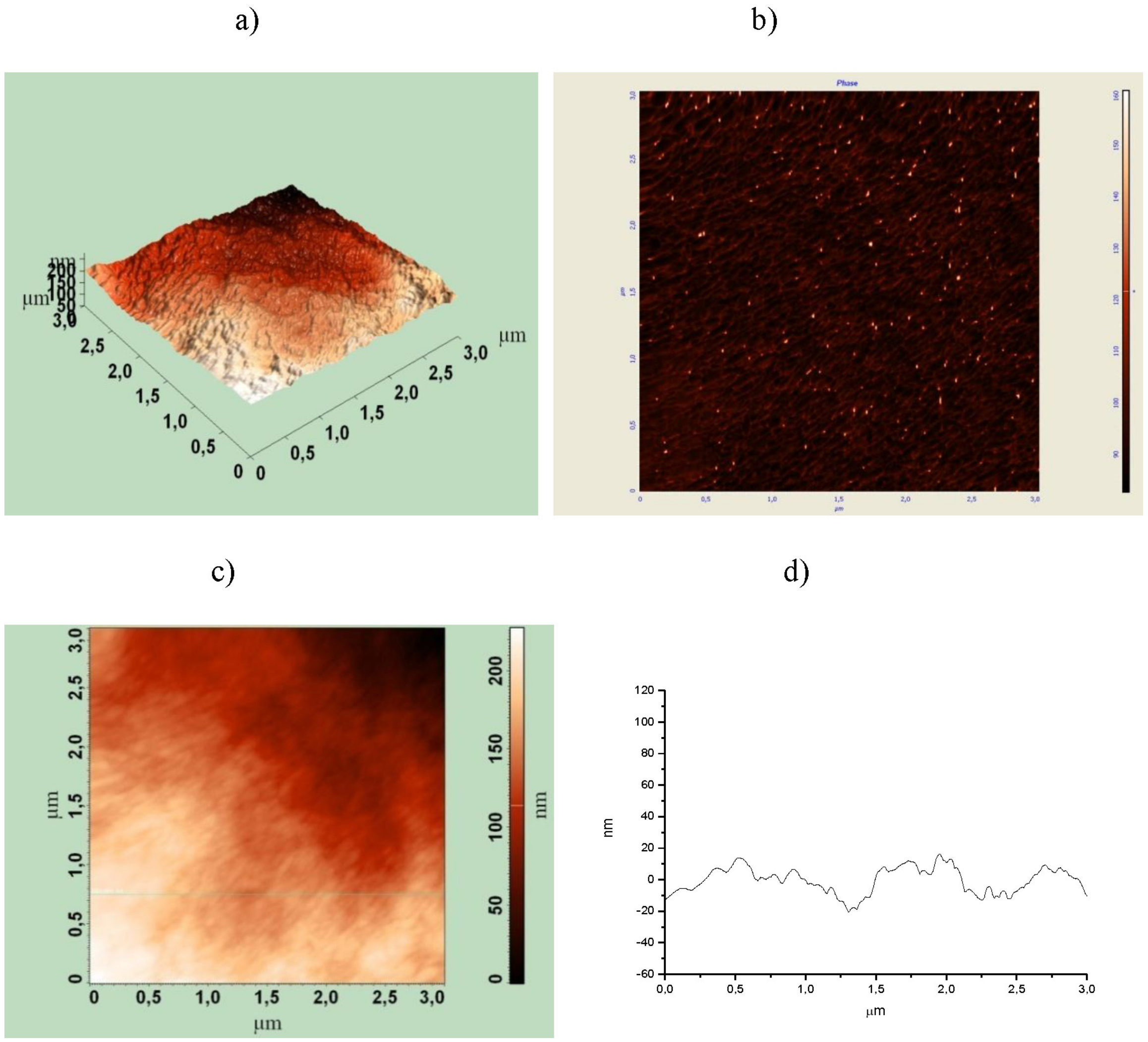

Fig. 2. AFM imaging of NCC-film surface (sample 1) under topography (a, c) and phase contrast conditions (b) under various scanning scales; (d) cross section profile along the line on pattern (c).

Sorption properties of cellulose obtained were evaluated on the basis of water sorption from a gas phase.

3. Results and discussions

The conditions of hydrolysis were as those described in Bondeson et al. (2006), with the following optimal parameters of the process: H_2SO_4 concentration – 63.5%, the concentration of the initial MCC – 10 g/100 ml, the temperature of hydrolysis – 44 °C and the time of the process – 130 min. By changing the temperature and hydrolysis time, we obtained 4 samples of NCC with various sulfate groups content. The alteration of hydrolysis conditions initiates the changes in other NCC characteristics. These are given in Table 1.

Analysis of the data obtained shows that under harder hydrolysis conditions (time and temperature) the degree of polymerization reduces and crystallinity index of the samples increases due to polymer chain breaking in amorphous areas of cellulose. According to X-ray diffraction analysis data, crystallite cross section calculated by Scherrer formula grows from 6.8 to 8.2 nm.

A major contributor to stability of the samples during thermodestruction is the presence of sulfate groups. NCC film decomposition proceeds via the two stages that are strongly pronounced on DTG curves (Fig. 1a). The destruction of the initial MCC takes place in one stage over a narrow temperature range 320–350 °C and is accompanied with a sizable drop in its mass (81%). The first step of NCC destruction appears to be the process of cellulose decomposition catalyzed by sulfate groups. It occurs at the temperatures lower than those of initial cellulose decomposition. The second step taking place at the temperatures higher than 370 °C appears to represent oxidation and destruction of carbon residue. The first pyrolysis step of sample 4 with the greatest sulfate group content proceeds at the temperatures 178 and 208 °C, corresponding to two endothermic peaks on DSC-curves (Fig. 1b, sample 4). Thus, the presence of sulfate groups in cellulose gives rise to a more complicated pattern of destruction, admittedly because of the formation and decomposition of various intermediate products.

DLS shows polydisperse character of particle distribution for all NCC samples. One can highlight two groups of particles with the size 30–40 nm and 200–400 nm respectively. The resulting hydrodynamic nanoparticle radii obtained by dynamic light scattering demonstrate that more rigid hydrolysis specifications (sample 4) are accompanied by the growth of an average size of the particle because of the dissolution of smaller particles of the first group.

AFM analysis revealed the different morphologies of the NCC-film surfaces with a small (sample 1) and a large (sample 4) amount of sulfate groups.

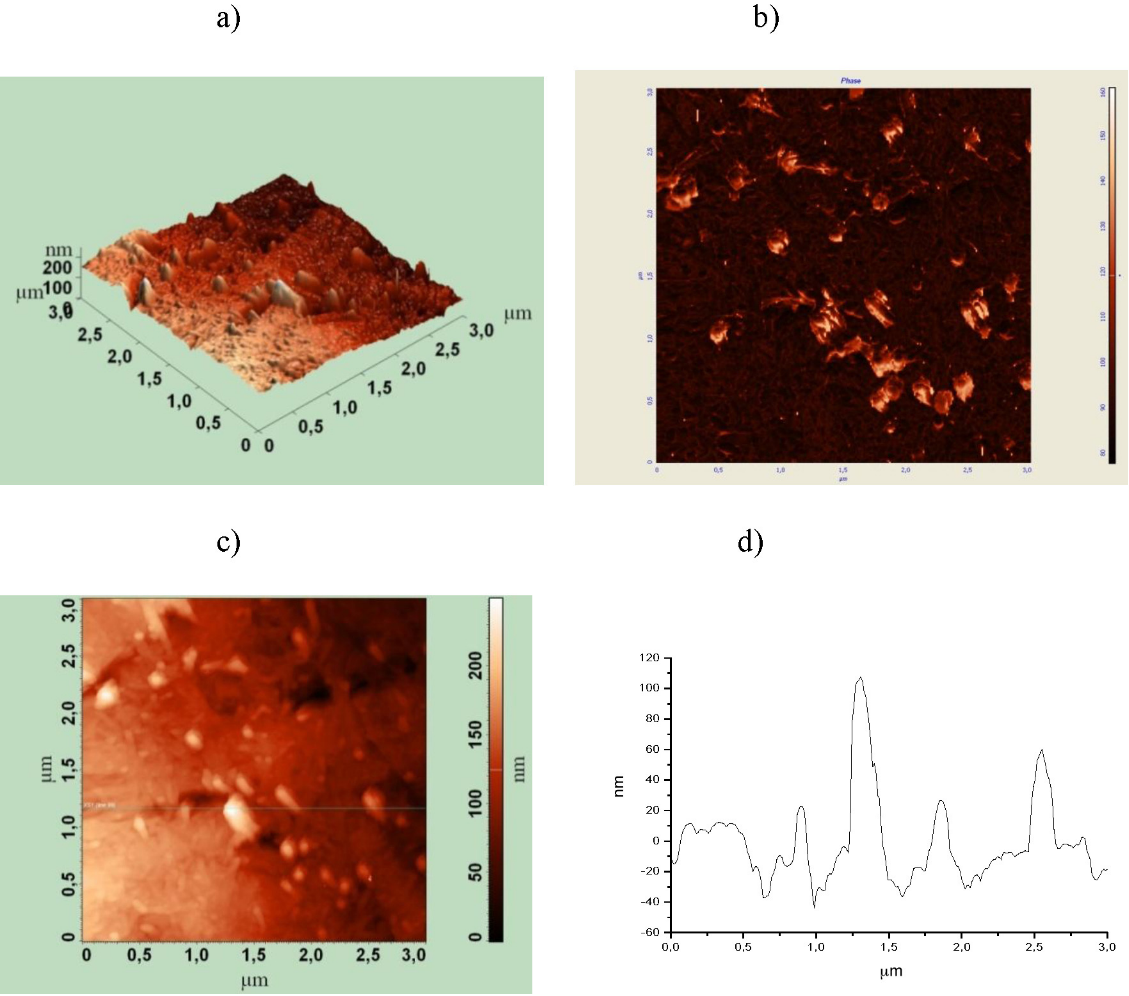

Fig. 3. AFM imaging of NCC sample (4) surface made under topography (a, c) and phase contrast conditions (b) under various scanning scales; (d) cross section profile along the line on pattern (c).

Analysis of AFM images made in topographical and phase contrast regime highlighted the roughness of the surface of NCC films with a small amount of sulfate groups (Fig. 2).

On the overall area of scanning of 15 × 15 μm one observes large enough surface topography fragments corresponding to big particle aggregates. At the same time, the image produced in phase contrast regime gives a uniform surface. Reduction of scanning area up to 3 μm^2 enables a finer structure of the surface with an ordered arrangement of particles to be distinguished (Fig. 2d). Root-mean-square roughness of the profile (Fig. 2d) equals 7 nm.

A different condition occurs (Fig. 3) on the surface of the film with high content of sulfate group (sample 4). One observes many aggregates on the surface with average sizes ranging from 50 to 100 nm in height and from 200 to 250 nm in width. Phase AFM images are presented as alternating dark and light zones. An average value of the surface roughness is 28 nm. It is much greater than for sample 1.

It has been shown earlier in Aulin et al. (2009), Jiang et al. (2010), and Winter et al. (2010) that one can produce NCC films possessing a smooth surface from NCC water suspensions of good dispersity and containing no clustered aggregates. It is achieved due to electrostatic repulsion between negatively charged NCC particles in water suspensions. In Winter et al. (2010) NCC film was formed on a rotating substrate from water dispersion of low concentration.

Slow water evaporation increases NCC concentration and, as a result, particle aggregation and the formation of a solid film with particle orientation relative to each other depending on their surface charge. Convergence of the like-charge particles maximizes repulsive forces. As a result, the aggregations of some particles take place perpendicular to the film surface (Fig. 3).

Adsorption properties of the resulting NCC-films were assessed in terms of their water adsorption from a gas phase. The difference in sorption capacity for NCC 1–3 samples as compared to that of

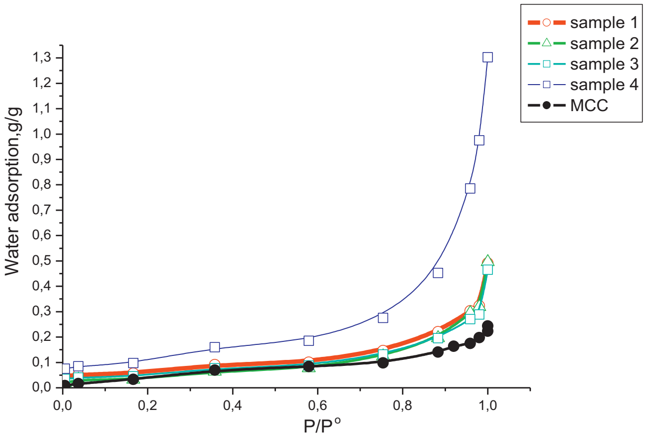

Fig. 4. Adsorption of water on NCC (1–4) and MCC samples.

MCC sample is mainly observed in the range of high P/Po values (Fig. 4).

Water sorption capacity of NCC sample 4 is much greater than that of MCC sample over the whole relative pressures range. As the index of crystallinity of samples 1–4 increases causing diminishing in the proportion of amorphous areas, as an outcome, the gain in water sorption capacity appears to be associated with the presence of sulfate groups in NCC samples that are able to act as adsorption sites. Besides, the morphology of the surface of NCC sample 4 becomes a contributory factor to increased capillary water condensation at high relative pressures.

4. Conclusion

Four samples of nanocrystalline cellulose with various sulfate groups content were obtained by changing acid hydrolysis conditions (time and temperature). Under harder hydrolysis conditions contents of sulfate groups grafting on cellulose crystallites surface increased, crystallinity index of the samples increased as well, and the degree of polymerization reduced. Dynamic light scattering experiments demonstrated polydisperse character of particle distribution for all NCC samples: more rigid hydrolysis specifications were accompanied by the growth of an average size of the particle because of the dissolution of smaller particles.

Properties of films derived by water evaporation from the aqueous NCC dispersions were studied by means of methods of atomic force microscopy, X-ray diffraction, thermogravimetric analysis, differential scanning calorimetry.

Surface morphology of the films changed as a function of contents of sulfate groups: with increasing sulfate groups content surface roughness increased and water adsorption enhanced.

The presence of sulfate groups catalyzed NCC films decomposition and hence reduced their thermal stability. Type of thermodestruction changed as a function of contents of sulfate groups as well. The destruction took place in two stages, and increasing sulfate groups content gave rise to a more complicated pattern of destruction, probably because of the formation and decomposition of various intermediate products.

References

Abitbol, T., Kloser, E., & Gray, D. G. (2013). Estimation of the surface sulfur content of cellulose nanocrystals prepared by sulfuric acid hydrolysis. *Cellulose*, *20*(2), 785–794, 10.1007/s10570-013-9871-0.

Aulin, C., Ahola, S., Josefsson, P., Nishino, T., Hirose, Y., Osterberg, M., et al. (2009). Nanoscale cellulose films with different crystallinities and mesostructures; their surface properties and interaction with water. *Langmuir*, *25*(13), 7675–7685. http://dx.doi.org/10.1021/la900323n

Bondeson, D., Mathew, A., & Oksman, K. (2006). Optimization of the isolation of nanocrystals from microcrystalline cellulose by acid hydrolysis. *Cellulose*, *13*(2), 171–180. http://dx.doi.org/10.1007/s10570-006-9061-4

Dong, X. M., Revol, J.-F., & Gray, D. G. (1998). Effect of microcrystallite preparation conditions on the formation of colloid crystals of cellulose. *Cellulose*, *5*(1), 19–32, 10.1023/A:1009260511939.

Elazzouzi-Hafraoui, S., Nishiyama, Y., Putaux, J. L., Heux, L., Dubreuil, F., & Rochas, C. (2008). The shape and size distribution of crystalline nanoparticles prepared by acid hydrolysis of native cellulose. *Biomacromolecules*, *9*(1), 57–65. http://dx.doi.org/10.1021/bm700769p

Gu, J., Catchmark, J. M., Kaiser, E. Q., & Archibald, D. D. (2013). Quantification of cellulose nanowhiskers sulfate esterification levels. *Carbohydrate Polymers*, *92*(2), 1809–1816. http://dx.doi.org/10.1016/j.carb.pol.2012.10.078

Habibi, Y., Lucia, L. A., & Rojas, O. J. (2010). Cellulose nanocrystals: Chemistry, self-assembly, and applications. *Chemical Reviews*, *110*(6), 3479–3500. http://dx.doi.org/10.1021/cr900339w

Jiang, F., Esker, A. R., & Roman, M. (2010). Acid-catalyzed and solvolytic desulfation of H_2SO_4-hydrolyzed cellulose nanocrystals. *Langmuir*, *26*(23), 17919–17925. http://dx.doi.org/10.1021/la1028405

Kim, U. J., Eom, S. H., & Wada, M. (2010). Thermal decomposition of native cellulose: Influence on crystallite size. *Polymer Degradation and Stability*, *95*(5), 778–781.

Lima, M. M., & Redouane, B. (2004). Rodlike cellulose microcrystals: Structure, properties, and application. *Macromolecular Rapid Communications*, *25*(7), 771–780.

Lu, P., & Hsieh, Y.-L. (2012). Preparation and characterization of cellulose nanocrystals from rice straw. *Carbohydrate Polymers*, *87*(1), 564–573. http://dx.doi.org/10.1016/j.carbpol.2011.08.022

Martínez-Sanz, M., Lopez-Rubio, A., & Lagaron, J. M. (2011). Optimization of the nanofabrication by acid hydrolysis of bacterial cellulose nanowhiskers. *Carbohydrate Polymers*, *85*(1), 228–236. http://dx.doi.org/10.1016/j.carbpol.2011.02.021

Rahimi, M., & Behrooz, R. (2011). Effect of cellulose characteristic and hydrolyze conditions on morphology and size of nanocrystal cellulose extracted from wheat straw. *International Journal of Polymeric Materials*, *60*(8), 529–541.

Thygesen, A., Oddershede, J., Lilholt, H., Thomsen, A. B., & Stahl, K. (2005). On the determination of crystallinity and cellulose content in plant fibres. *Cellulose*, *12*(6), 563–576. http://dx.doi.org/10.1007/s10570-005-9001-8

Wang, N., Ding, E., & Cheng, R. (2007). Thermal degradation behaviors of spherical cellulose nanocrystals with sulfate groups. *Polymer*, *48*(12), 3486–3493. http://dx.doi.org/10.1016/j.polymer.2007.03.062

Winter, H. T., Cerclier, C., Delorme, N., Bizot, H., Quemener, B., & Cathala, B. (2010). Improved colloidal stability of bacterial cellulose nanocrystal suspensions for the elaboration of spin-coated cellulose-based model surfaces. *Biomacromolecules*, *11*(11), 3144–3151. http://dx.doi.org/10.1021/bm100953f